Semiconductor Physics, Quantum Electronics & Optoelectronics, 2022. V. 25, No 4. P. 362-371.

Semiconductor physics

Characterization of adsorption properties inherent to zirconia dioxide for different positions of yttrium in the ZrO_2–Y_2O_3 lattice

S.I. Lyubchyk[1,2], S.B. Lyubchyk[1,2], A.I. Lyubchyk[2]

[1]*REQUIMTE, NOVA School of Science and Technology, University New of Lisbon, 2829-516 Caparica, Portugal*
[2]*DeepTechLab, Universidade Lusófona, Campo Grande, 376, 1749-024 Lisboa, Portugal*
E-mail: p6193@ulusofona.pt

Abstract. Presented in this paper is theoretical studying redistribution of electric charges in the layer of a tetragonal plate of yttrium-stabilized zirconia based on the position of yttrium atom in the crystal lattice for both dry and humid ambient atmosphere. The density functional theory with local density approximation (DFT-LDA) has been employed for this modelling. Calculations have been performed for layer-by-layer electron density distribution over the thickness of an infinite plate 001 of yttrium-stabilized tetragonal zirconium dioxide, which show that a change in the position of stabilizing yttrium atom and its symmetry in the layer leads to changing the total energy of zirconium dioxide both for the dry 001 surface and for the hydrated one. It has been ascertained that the surface charge density for the 001-surface of an infinite tetragonal zirconia plate increases in proportion to the degree of hydration.

Keywords: zirconium dioxide, yttrium, local potential, total energy, hydrated surface.

https://doi.org/10.15407/spqeo25.04.362
PACS 68.43.-h, 71.15.Dx, 73.20.Hb

Manuscript received 31.08.22; revised version received 14.10.22; accepted for publication 14.12.22; published online 22.12.022.

1. Introduction

Currently, various devices that can convert the potential energy of atmospheric humidity into an electrical form at the micro-level are being actively developed in the world [1–3]. One of the materials used to create such devices is yttria-stabilized zirconium oxide (YSZ) that can exhibit proton conductivity in a humid atmosphere [4–6]. Moreover, the possibility of creating multilayer barrier structures based on compacted nano-dispersed YSZ by using the potential of atmospheric moisture as a new energy source was demonstrated in [7–9]. However, the features of the influence of yttrium oxide as a stabilizer of zirconium oxide are still the subject of discussion. It should be noted that, under real conditions, not only oxygen, zirconium, or yttrium, but also other compounds from the surface atmosphere, namely hydrogen or water, can be adsorbed on the ZrO_2 surface [10–13]. All this shows that the question of actual structure inherent to the surface of zirconium dioxide is nontrivial and will depend on the surrounding atmosphere, as in the case of surfaces in other oxides [14–16]. Of particular interest is the relation between the electrical phenomena accompanying interaction of water with the surface of zirconium dioxide stabilized by yttrium oxide and the position of the Y atom on the surface of ZrO_2.

The purpose of this work is a theoretical study of redistribution inherent to electric charges in the layers of a tetragonal plate of yttrium-stabilized zirconium dioxide depending on the position of yttrium atom in the crystal lattice for the cases of dry or humid atmosphere.

2. Energy contribution during interaction of water with the surface

In this work, quantum-mechanical evaluation of the influence of position inherent to yttrium in a tetragonal zirconium dioxide plate on the total energy of the system and its components was carried out. Simulation was performed within the framework of density functional theory (DFT) [17–19]. DFT was used to describe interaction of a fermionic system in terms of the three-dimensional density of electrons, and not in terms of their multi-dimensional wave functions. The calculations performed by the DFT method for zirconium dioxide were based on an approximation of the so-called exchange-correlation potential. The method of choosing this local potential in the form of the potential of homogeneous electron gas, the so-called local density approximation (LDA), was used. DFT modelling [18] was carried out using the *abinit-tool* nano-HUB [20–22] (ABINIT [23]).

© 2022, V. Lashkaryov Institute of Semiconductor Physics, National Academy of Sciences of Ukraine

Table. Coordinates of atoms nuclei.

Atom	τ_a	τ_b	τ_c	Atom	τ_a	τ_b	τ_c
H	19.319/32	0.704/2	0	Y11(Zr)	11/32	1/4	1/4
H	19.319/32	1.296/2	0	Zr	11/32	3/4	3/4
O	18.408/32	1/2	0	O	9.592/32	0	0
O	17.592/32	0	0	O	9.592/32	1/2	1/2
O	17.592/32	1/2	1/2	O	10.408/32	1/2	0
Zr	17/32	3/4	1/4	O	10.408/32	0	1/2
Zr(Y17)	17/32	1/4	3/4	Zr	9/32	3/4	1/4
O	15.592/32	0	0	Zr(Y9)	9/32	1/4	3/4
O	15.592/32	1/2	1/2	O	7.592/32	0	0
O	16.408/32	1/2	0	O	7.592/32	1/2	1/2
O	16.408/32	0	1/2	O	8.408/32	1/2	0
Zr(Y15)	15/32	1/4	1/4	O	8.408/32	0	1/2
Zr	15/32	3/4	3/4	Zr(Y7)	7/32	1/4	1/4
O	13.592/32	0	0	Zr	7/32	3/4	3/4
O	13.592/32	1/2	1/2	O	5.592/32	0	0
O	14.408/32	1/2	0	O	5.592/32	1/2	1/2
O	14.408/32	0	1/2	O	6.408/32	1/2	0
Zr	13/32	3/4	1/4	O	6.408/32	0	1/2
Zr(Y13)	13/32	1/4	3/4	Zr	5/32	3/4	1/4
O	12.408/32	1/2	0	Zr(Y5)	5/32	1/4	3/4
O	12.408/32	0	1/2	O	4.408/32	1/2	0
O	11.592/32	0	0	O	4.408/32	0	1/2
O	11.592/32	1/2	1/2	Y11(Zr)	11/32	1/4	1/4

To study the features of hydration of the 001 surface of tetragonal zirconium dioxide, an atomic model of a cell typical for the zirconium dioxide plate was constructed. A rectangular parallelepiped with the sides $\vec{a}\times\vec{b}\times\vec{c}$, of a = 39.06436757846 boron, b = 9.64728151559 boron, c = 9.64728151559 boron (1 boron = 0.5291772108 angstrom) was chosen as a cell. The basis vector of the nucleus of an atom s in a cell can be written as $\vec{\tau}_s = \tau_a^s\vec{a} + \tau_b^s\vec{b} + \tau_c^s\vec{c}$. The cell for modelling the zirconium dioxide hydrated 001 surface consisted of 45 atoms (13 zirconium atoms, 1 yttrium atom, 29 oxygen atoms and 2 hydrogen atoms) with the coordinates given in Table (Fig. 1).

Almost all dynamic properties of the lattice of solids can be obtained by knowing the total energy (E_{tot}) of the solid as a function of the position of the atoms.

The term "total energy" as used herein refers to the total energy of a system of "frozen" nuclei. We neglect the kinetic energy of the nuclei.

Three approximations were used to calculate E_{tot}:

(i) an adiabatic (Born–Oppenheimer) approximation, in which the electrons are in the ground state with respect to the instantaneous position of the nuclei and the ground state energy (*e.g.*, E_{tot}) that is the effective potential for nuclear motions,

(ii) the local density functional approximation, in which the exchange-correlation interactions of electrons are approximated by the local density functional, and

(iii) pseudopotential approximation, in which interaction of valence electrons with the ionic skeleton of an atom is modelled by using pseudopotentials.

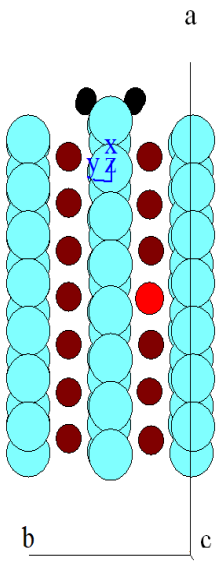

Fig. 1. Cell ZrO_2 with Y (red – fourth left) and H_2O. (Color online)

The total energy of a crystal in the theory of pseudopotentials can be written as follows:

$$E_{tot} = E_{kin} + E_{loc} + E_{nonloc} + E_{corr-core} + E_{\mathrm{H}} + E_{xc} + E_{\mathrm{Ew}}, \quad (1)$$

where E_{kin} corresponds to the kinetic energy of valence electrons.

The energy of interaction of valence electrons with an ionic nucleus consists of E_{loc} – local energy, E_{nonloc} – non-local energy, $E_{corr-core}$ – ion core correction energy.

The energy of interaction of valence electrons with each other consists of E_{H} – Hartree energy of valence electrons, E_{xc} – exchange-correlation energy of valence electrons.

Finally, classical electrostatic Coulomb interaction of the ionic cores of lattice atoms with each other is denoted E_{Ew} – Ewald's energy.

The component of the local electron-ion interaction of the total energy of the crystal cell in the theory of pseudopotentials can be presented as follows:

$$E_{loc} = \sum_s \int d\vec{r} \rho_v^{PP}(\vec{r}) V_{s-ion,loc}(\vec{r} - \vec{\tau}_s), \quad (2)$$

where $\vec{\tau}_s$ – the basis vector of the atom s in the cell, and $V_{s-ion,loc}(\vec{r} - \vec{\tau}_s)$ – local pseudopotential of the ionic skeleton in this atom; $\rho_v^{PP}(r) = \sum_l n_l \left| R_l^{PP}(r) \right|^2$ – valence pseudodensity.

The component of nonlocal electron-ion interaction of the total energy of a crystal cell in the theory of pseudopotentials can be expressed as follows:

$$E_{nonloc} = \sum_{l,s} n_l \int d\vec{r} R_l^{*PP}(\vec{r}) V_{nonloc,l}^s(\vec{r} - \vec{\tau}_s) R_l^{PP}(\vec{r}). \quad (3)$$

The symbols n_l and $R_l^{PP}(\vec{r})$, respectively, are the population and pseudowave function for the one-electron state l.

$V_{nonlocl}^s(\vec{r} - \vec{\tau}_s)$ depends on the angular momentum l of the nonlocal pseudopotential for the ionic core of the atom s in the cell.

The results of simulation performed for local and nonlocal energy for a plate of tetragonal zirconium dioxide without water and with it on the 001 surface are shown in Fig. 2a, b. As can be seen from Fig. 2a, since yttrium approaches the zirconium dioxide surface, the negative value of the local energy increases in its absolute value. Addition of water to one of the surfaces reduces the local energy (Fig. 2a). At the same time, with yttrium approach to the zirconium surface, the positive value of the nonlocal energy changes non-monotonically. Addition of water to one of the surfaces increases the nonlocal energy (Fig. 2b).

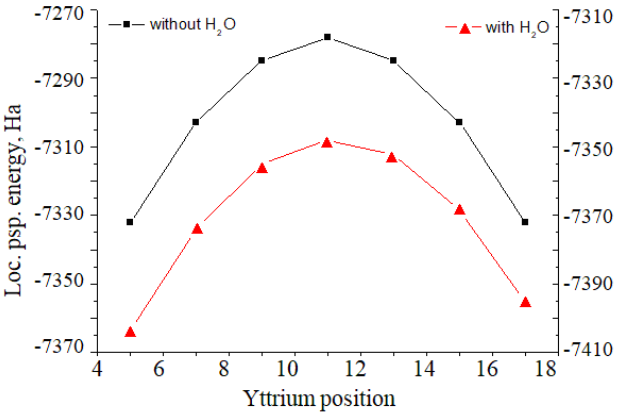

a)

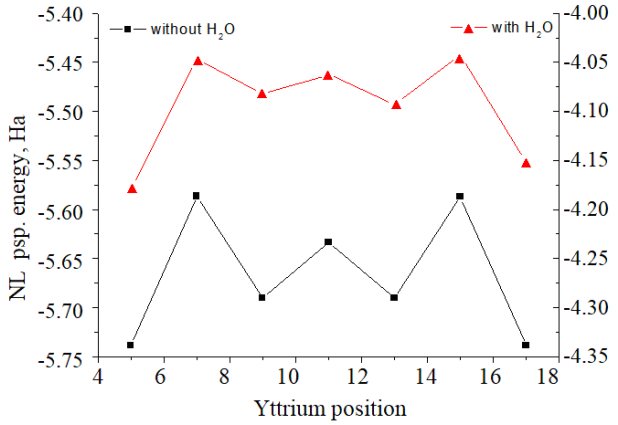

b)

Fig. 2. Variation of local energy under hydration of the zirconia 001 surface for different yttrium positions (a) and change of the nonlocal energy (b).

The correction energy for the ionic nucleus of all the atoms of the cell is written as

$$E_{corr-core} = \sum_s \int d\vec{r}\rho_v^{PP}(\vec{r}) \begin{bmatrix} V_{xc}\left(\left[\rho_v^{PP}\right], \vec{r} - \vec{\tau}_s\right) - \\ -V_{xc}\left(\left[\rho_v^{PP} + \rho_{s-core}^{AE}\right], \vec{r} - \vec{\tau}_s\right) \end{bmatrix}$$

where $\vec{\tau}_s$ is the basis vector for the atom s in the source, and ρ_{core}^{AE} – entire electron density of the core belonging to the ion of this atom; $\rho_v^{PP}(r) = \sum_l n_l \left|R_l^{PP}(r)\right|^2$ – valence pseudodensity, V_{xc} – exchange-correlation pseudopotential.

The results of modelling the correction energy of ion core for the tetragonal zirconium dioxide plate without water and with it on the 001 surface showed that in the case when the yttrium atom replaces the zirconium one on the surface, as well as when water is added, the positive value of this component does not change.

The Hartree energy of the valence electrons of each cell is:

$$E_{\mathrm{H}}\left[\rho_v^{PP}\right] = \frac{1}{2}\int \rho_v^{PP}(\vec{r}) V_{\mathrm{H}}^{PP}\left(\rho_v^{PP}(\vec{r})\right) d\vec{r} \,. \quad (5)$$

Here, $\rho_v^{PP}(r) = \sum_l n_l \left|R_l^{PP}(r)\right|^2$ is the valence pseudodensity, V_{H}^{PP} – valence Hartree pseudopotential.

In the local density functional approximation, the exchange-correlation energy of valence electrons $E_{xc}\left[\rho_v^{PP}\right]$ can be presented for each cell as:

$$E_{xc}\left[\rho_v^{PP}\right] = \int \rho_v^{PP}(\vec{r}) V_{xc}\left(\rho_v^{PP}(\vec{r})\right) d\vec{r} \,, \quad (6)$$

where $\rho_v^{PP}(r) = \sum_l n_l \left|R_l^{PP}(r)\right|^2$ is the valence pseudo-density, V_{xc} – exchange-correlation pseudopotential.

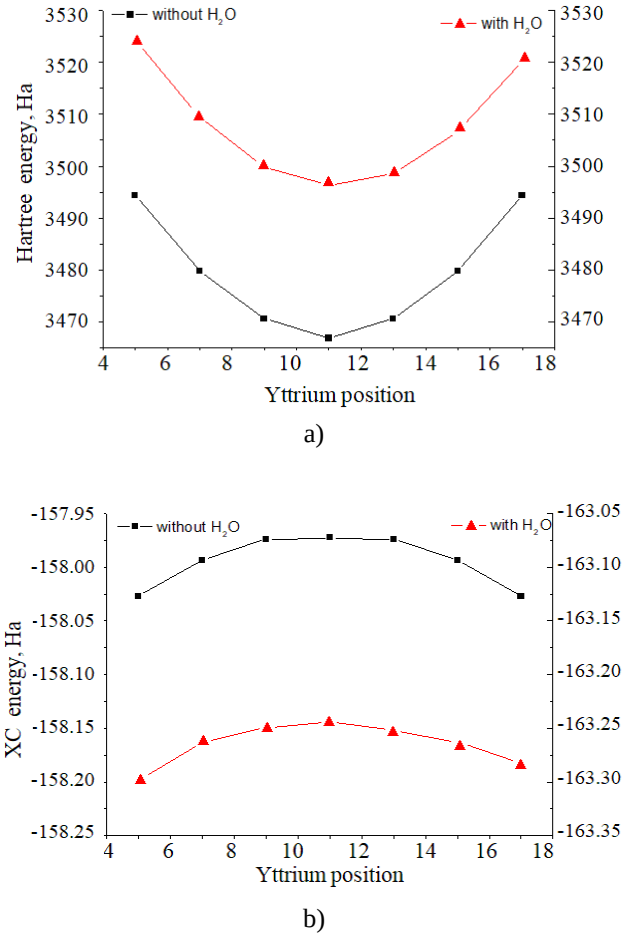

Fig. 3. Change in the Hartree energy after hydration of 001 surface of tetragonal zirconia for different yttrium positions (a) and change in the exchange-correlation energy during hydration (b).

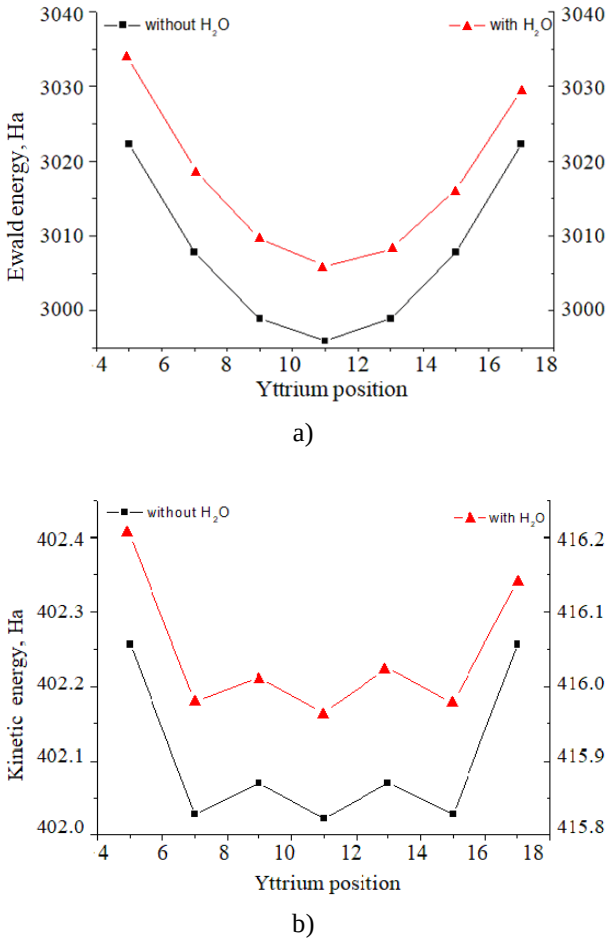

Fig. 4. Variation of Ewald's energy when hydrating the 001 surface of zirconia for different yttrium positions (a), variation of kinetic energy (b).

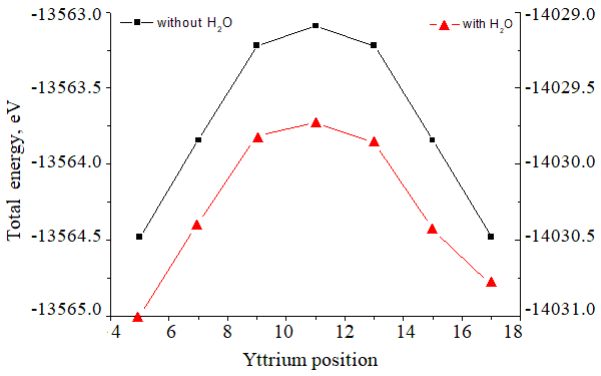

Fig. 5. Variation of total energy during hydration of the 001 surface of zirconia for various yttrium positions.

The results of modelling the Hartree energy and the exchange-correlation energy of valence electrons for a plate of tetragonal zirconium oxide without and with water on the 001 surface are shown in Fig. 3. As can be seen from Fig. 3a, when yttrium is located closer to the zirconium oxide surface, the positive value of the Hartree energy increases monotonically. The dependence of the Hartree energy on the position of yttrium has a minimum at the central position of yttrium, and the addition of water to one of the surfaces increases the Hartree energy (Fig. 3a). As can be seen from Fig. 3b, when yttrium is located closer to the zirconium dioxide surface, the negative value of the exchange-correlation energy of valence electrons increases in its absolute value, forming an energy maximum in the central position of yttrium (Fig. 3b). Addition of water to one of the surfaces increases the exchange-correlation energy (Fig. 3b).

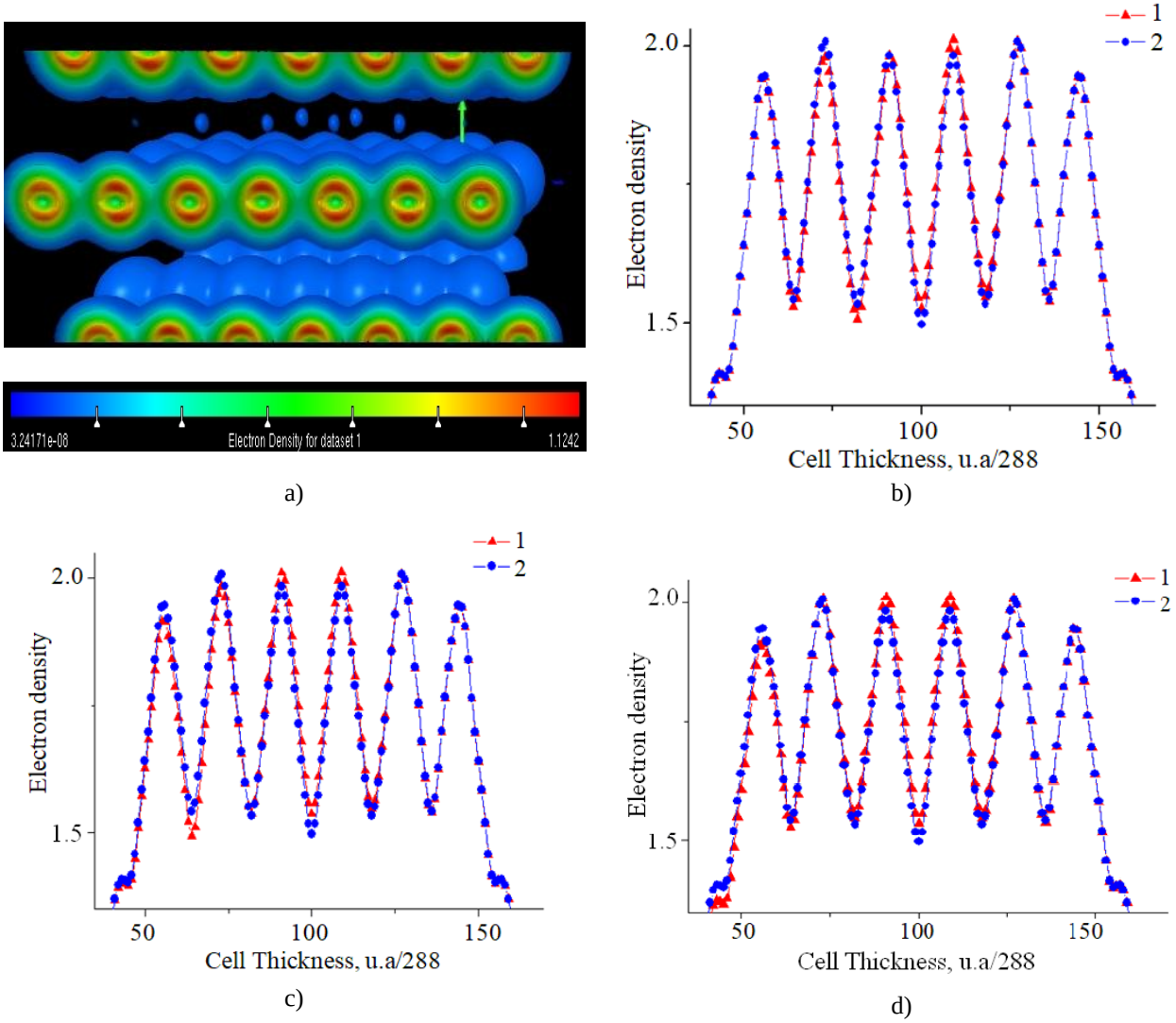

Fig. 6. The electronic density of zirconia cell calculated using the DFT method (a). Comparison of the layered distribution of the electron density at the central and subcentral positions of yttrium (b), at the central and near-surface positions of yttrium (c), at the central and surface positions of yttrium (d). *1* – different positions of yttrium in the cell (Y9, Y7, Y5); *2* – central position of yttrium in the cell (Y11).

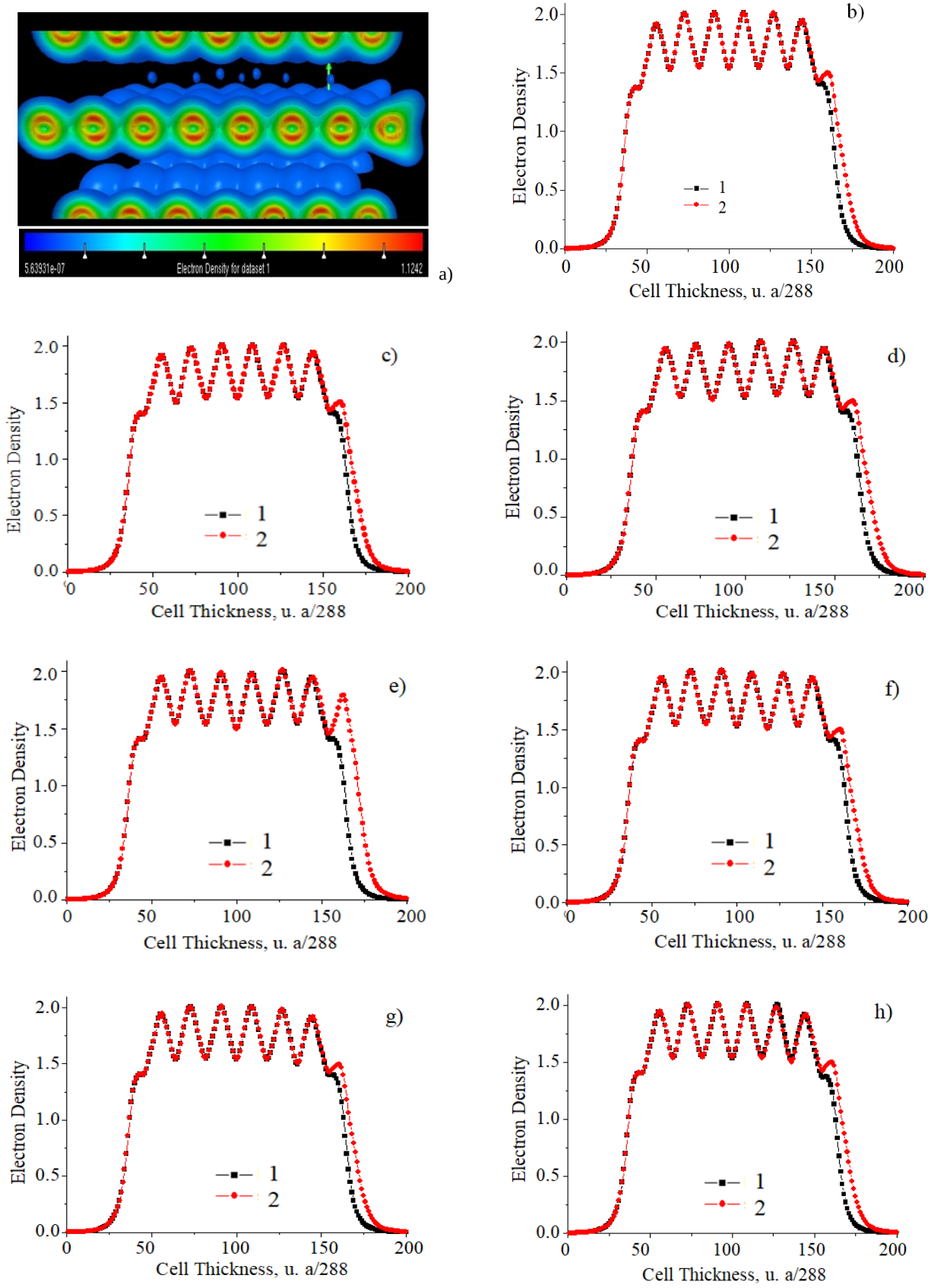

Fig. 7. Distribution of the electron density for tetragonal zirconia with and without water molecules at the 001 surface for different positions of the yttrium atom in the cell: Y5, Y7, Y9, Y11, Y13, Y15, Y17 (b–h). *1* – position of the yttrium atom without water; *2* – position of the yttrium atom with water.

It is very difficult to calculate the Coulomb energy of a system of ions by direct summation in real space, since the Coulomb interaction is long-ranged.

In reciprocal space, the Coulomb interaction is also long-range, so the problem cannot be solved by summation in reciprocal space, too. Ewald [24–26] developed the fast convergence method for performing Coulomb summation over periodic lattices.

$$E_{\mathrm{Ew}} = \sum_{s,t} \frac{Z_s Z_t}{\left|\vec{\tau}_s - \vec{\tau}_t\right|}. \qquad (7)$$

The results of modelling the Coulomb ion-ion interaction for a plate of tetragonal zirconium dioxide without water and with it on the 001 surface are shown in Fig. 4a. As can be seen, when yttrium is located closer to the zirconium dioxide surface, the positive value of this component increases, forming a minimum in the central position of yttrium. Adding water to one of the surfaces increases the energy.

The kinetic energy was calculated as follows:

$$E_{kin} = \sum_{l} n_l \int d\vec{r} R_l^{*PP}(\vec{r}) \left(-\nabla^2\right) R_l^{PP}(\vec{r}), \qquad (8)$$

where n_l and $R_l^{PP}(\vec{r})$ are, respectively, the population and pseudowave function for the one-electron state *l*.

The results of modelling the kinetic energy for a plate of tetragonal zirconium dioxide without water and with it on the surface 001 are shown in Fig. 4b. As can be seen, when yttrium is located closer to the zirconium dioxide surface, the positive value of this component is nonmonotonic. Addition of water to one of the surfaces resulted in an increase in energy.

Fig. 5 shows the change in the total energy of zirconia with the hydrated 001 surface (red squares) and without hydration (black squares) for different positions of the yttrium atom.

As can be seen from Fig. 5, the maximum of the total energy is observed when yttrium is in the center. Adding water to one of the surfaces reduces the overall energy.

Let us consider how the layer-by-layer distribution of electron density changes depending on the position of yttrium during hydration of the symmetrical surface Zr-O 001 of an infinite seven-layer plate of tetragonal zirconium oxide stabilized by yttrium.

As a result of modelling the plate of tetragonal zirconia stabilized with yttrium (yttrium in the central position), the electron density was obtained in the case of a dry, symmetrical atmosphere, which is shown in Fig. 6a.

Being based on the obtained distribution of the electron density over the cell volume, it is possible to calculate the layer-by-layer distribution of the electric charge, when the position of yttrium changes is compared to the central location in the cell. We will consider the following positions of yttrium: central (Y11) (Fig. 6b to 6d, curve *2*), near central (Y9) (Fig. 6b, curve *1*), near-surface (Y7) (Fig. 6c, curve *1*) and surface (Y5) (Fig. 6d, curve *1*) (see Table). It should be noted that the latter position of yttrium no longer applies to the symmetrical surfaces of the plates. Figs 6b to 6d show the dependences of the layer-by-layer electron density distribution depending on the cell thickness for different positions of yttrium in the cell. As can be seen from Figs 6b–6d, the position of yttrium in the cell has practically no effect on the electron density distribution in the cell in the case of a dry symmetrical atmosphere.

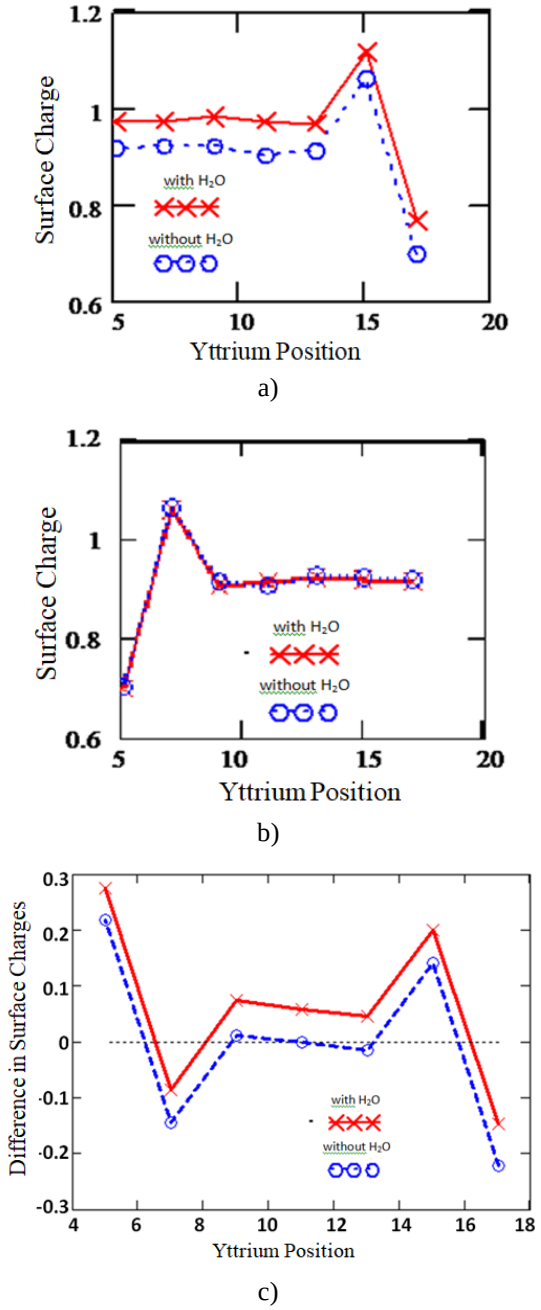

Fig. 8. Variation of the surface charge for the moistened layer (a) and dry layer (b) of the 001 surface of tetragonal zirconia at different yttrium positions positions relative to the moistened layer. The change in the difference in the surface charges of the moistened and dry surface of 001 tetragonal zirconia at different yttrium positions with respect to the water-moistened layer (c).

As a result of modelling the hydration of a plate of tetragonal zirconium dioxide stabilized with yttrium (yttrium in the central layer), the electron density presented in Fig. 7a was obtained.

Figs 7b–7h shows the electron density distribution of yttrium-stabilized tetragonal zirconium dioxide with and without water molecules on the 001 surface for different positions of the yttrium atom in the cell:
(Y5) – the yttrium atom is in the dry surface layer (7b), (Y7) – in the dry near-surface layer (Fig. 7c), (Y9) – in the subcentral layer on the dry side (Fig. 7d), (U11) – in the central layer (Fig. 7e), in (Y13) – the subcentral layer with hydrated sides (Fig. 7f), (Y15) in the hydrated surface layer (Fig. 7g) and (Y17) – in the hydrated surface layer (Fig. 7h). As can be seen from Figs 7b to 7h, for any position of the yttrium atom in a cell with the thickness less than 150 u.a/288, there are practically no differences in the layer-by-layer distribution of the electron density inherent to tetragonal zirconium dioxide for dry and hydrated surfaces. However, as the cell thickness increases above 150 u.a/288, the layer-by-layer distribution of the electron density for dry and wet surfaces changes. In this case, the maximum differences in the layer-by-layer distribution of the electron density for dry and hydrated surfaces arise, when the yttrium atom is located in the central layer (Y11).

Figs 8a, 8b and 8c show the results of calculations of changes in the surface charge of the hydrated (Fig. 8a) and dry (Fig. 8b) surface layer, as well as changes in the difference in surface charges on the wet and hydrated surfaces (Fig. 8c) of 001 tetragonal zirconia at various positions of yttrium relatively to the layer (see Table).
The change in the surface density of the electric charge for a combination of dry and hydrated surface layers of a tetragonal zirconium dioxide plate, depending on the different degree of hydration of the 001 surfaces of the dioxide, is shown in Fig. 9.

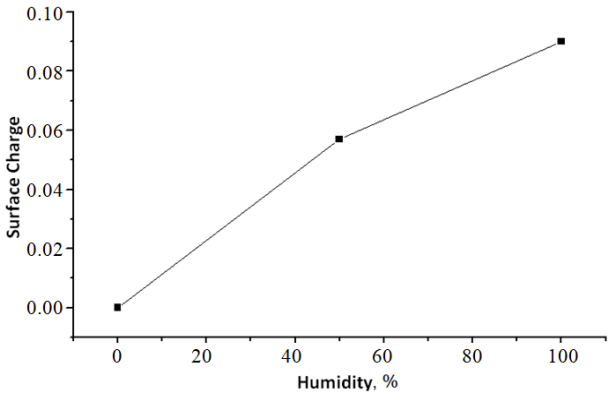

Fig. 9. Variation of the surface density for the electric charge difference of the combination of moistened surface layers of a plate of tetragonal zirconium dioxide as a function of the difference in the degree of moistening the 001-surface of dioxide.

As can be seen from Fig. 9, the surface charge density for the zirconia 001 surface increases in proportion to the degree of wetting. The proportionality factor is approximately equal to 0.35 mC/(cm^2%).

3. Conclusions

Calculations of the layer-by-layer electron density distribution over the thickness of an infinite plate 001 of yttrium-stabilized tetragonal zirconium dioxide showed that a change in the position of the stabilizing yttrium atom and its symmetry in the layer lead to a change in the total energy of zirconium dioxide both for the dry 001 surface and for the hydrated one. In this case, the minimum electron concentration is observed in the layer containing stabilizing yttrium. This distribution of electron density over the thickness of wafer on yttrium-stabilized tetragonal zirconium dioxide will affect the features of the electrical conductivity in each layer.

The surface charge density for the 001 surface of an infinite tetragonal zirconia plate increases in proportion to the degree of hydration. The proportionality factor is equal approximately 0.35 mC/(cm^2%).

Acknowledgements

This project has been supported by funding from the European Union's Horizon 2020 research and innovation program in accord to the Marie Sklodovska-Curie grant agreement 871284.

References

1. Liu X., Gao H., Ward J.E. *et al.* Power generation from ambient humidity using protein nanowires. *Nature.* 2020. **578**. P. 550–554. https://doi.org/10.1038/s41586-020-2010-9.
2. Shen D., Duley W.W., Peng P. *et al.* Moisture-enabled electricity generation: From physics and materials to self-powered applications. *Adv. Mater.* 2020. **32**(52). P. 2003722. https://doi.org/10.1002/adma.202003722.
3. Yang L., Nandakumar D.K., Miao L. *et al.* Energy harvesting from atmospheric humidity by a hydrogel-integrated ferroelectric-semiconductor system. *Joule.* 2020. **4**. P. 176. https://doi.org/10.1016/j.joule.2019.10.008.
4. Anselmi-Tamburini U., Maglia F., Chiodelli G. *et al*. Enhanced low-temperature protonic conductivity in fully dense nanometric cubic zirconia. *Appl. Phys. Lett.* 2006. **89**. P. 3116. https://doi.org/10.1063/1.2360934.
5. Dawson J.A., Tanaka I. Significant reduction in hydration energy for yttria stabilized zirconia grain boundaries and the consequences for proton conduction. *Langmuir*. 2014. **30**. P. 10456. https://doi.org/10.1021/la501860k.
6. Guo X., Yuan R.Z. On the grain boundaries of ZrO_2-based solid electrolyte. *Solid State Ionics*. 1995. **80**. P. 159. https://doi.org/10.1016/0167-2738(95)00131-O.

7. Bacherikov Y.Y., Lytvyn P.M., Mamykin S.V. *et al*. Current transfer processes in a hydrated layer localized in a two-layer porous structure of nanosized ZrO_2. *J. Mater. Sci.: Mater. Electron*. 2022. **33**. P. 2753. https://doi.org/10.1007/s10854-021-07481-2.
8. Bacherikov Yu.Yu., Okhrimenko O.B. Principles of creating the devices that are able to control the current flow in the second class conductors. *SPQEO*. 2022. **25**. P. 137. https://doi.org/10.15407/spqeo25.02.137.
9. Bacherikov Yu.Yu., Okhrimenko O.B., Goroneskul V.Yu. *et al*. The model of potential barrier appearing in a hydrolayer localized in a two-layer porous nanostructure. *SPQEO*. 2021. **24**. P. 288. https://doi.org/10.15407/spqeo24.03.288.
10. Chaopradith D.T., Scanlon D.O., Catlow C.R.A. Adsorption of water on yttria-stabilized zirconia. *J. Phys. Chem. C*. 2015. **119**. P. 22526. https://doi.org/10.1021/acs.jpcc.5b06825.
11. Eichler A., Kresse G. First-principles calculations for the surface termination of pure and yttria-doped zirconia surfaces. *Phys. Rev. B.* 2004. **69**. P. 045402. https://doi.org/10.1103/PhysRevB.69.045402.
12. Merle-Mejean T., Barberis P., Ben Othmane S. *et al*. Chemical forms of hydroxyls on/in zirconia: An FT-IR study. *J. Europ. Ceram. Soc.* 1998. **18**. P. 1579. https://doi.org/10.1016/S0955-2219(98)00080-6.
13. Eder D., Kramer R. The stoichiometry of hydrogen reduced zirconia and its influence on catalytic activity. Part 1: Volumetric and conductivity studies. *Phys. Chem. Chem. Phys.* 2002. **4**. P. 795. https://doi.org/10.1039/B109887J.
14. Wang X.-G., Chaka A., and Scheffler M. Effect of the environment on a-Al_2O_3 (0001) surface structures. *Phys. Rev. Lett.* 2000. **84**. P. 3650. https://doi.org/10.1103/PhysRevLett.84.3650.
15. Reuter K. and Scheffler M. Composition, structure, and stability of RuO_2 (110) as a function of oxygen pressure. *Phys. Rev. B.* 2002. **65**. P. 035406. https://doi.org/10.1103/PhysRevB.65.035406.
16. Sun Q., Reuter K. and Scheffler M. Effect of a humid environment on the surface structure of RuO_2 (110). *Phys. Rev. B*. 2003. **67**. P. 205424. https://doi.org/10.1103/PhysRevB.67.205424.
17. Muhammad S., Hussain S.T., Waseem M. *et al*. Surface charge properties of zirconium dioxide. *Iran. J. Sci. & Technol*. 2012. **A4**. P. 481. https://doi.org/10.22099/ijsts.2012.2110.
18. Hohenberg P., Kohn W. Inhomogeneous electron gas. *Phys. Rev. B.* 1964. **136**. P. 864. https://doi.org/10.1103/PhysRev.136.B864.
19. Tokiy N.V., Savina D.L., Tokiy V.V. Materials of Mediterranean-East-Europe Meeting "Multi-functional Nanomaterials (NanoEuroMed 2011)". Ukraine, Uzhgorod, 2011. P. 165–166.
20. Nanohub tools at http://www.nanohub.org.
21. Klimeck G., McLennan M., Brophy S. *et al*. nanoHUB.org: Advancing Education and Research in Nanotechnology. *IEEE Computers in Engineering and Science*. 2008. **10**. P. 17–23. https://doi.org/10.1109/MCSE.2008.120.
22. Palaria A., Wang X., Haley B. *et al*. ABINIT on nanoHUB. https://doi.org/10.4231/D3XS5JH8J.
23. http://www.abinit.org
24. Ewald P.P. Zur Begründung der Kristalloptik. *Ann. Phys*. 1917. **359**. P. 519. https://doi.org/10.1002/andp.19173592305.
25. Ewald P.P. Zur Begründung der Kristalloptik. *Ann. Phys*. 1917. **359**. P. 557. https://doi.org/10.1002/andp.19173592402.
26. Ewald P.P. Die Berechnung optischer und elektrostatischer Gitterpotentiale. *Ann. Phys*. 1921. **369**. P. 253. https://doi.org/10.1002/andp.19213690304.

Authors and CV

Prof. **Andriy Lyubchyk** holds a PhD in Chemical Engineering, specialized in the fields of alternative energy and advanced materials research. His fields of expertise are nanomaterials, nanotechnology and electronics. Current research interests are in the field of processing nanomaterials based photovoltaic materials and devices; plasmonic materials and microfluidics. https://orcid.org/0000-0002-8883-8283

Prof. **Svitlana Lyubchyk** holds a PhD in Chemistry. Research work of Prof. Lyubchyk is diverse and multi-disciplinary, with core areas in green chemistry, carbon nanomaterials, life sciences and environmental engineering. The fields of expertise are nanomaterials, nanotechnology and environmental engineering. Current research interests are in the field of synthesis and characterization of carbon materials, nanomaterials and ceramic based composites.
https://orcid.org/0000-0003-3194-4058;
e-mail: s.lyubchyk@fct.unl.pt; p5322@ulusofona.pt

Prof. **Sergiy Lyubchyk** holds a PhD in Chemical Engineering, specialized in the fields of alternative energy and advanced materials research. He has strong experience in development of sustainable green products and processes. Current research interests are in the field of advanced nanomaterials development, design and application, photochemistry of the advanced composites based on nanometals oxides and fullerenes.
https://orcid.org/0000-0001-6323-938;
e-mail: se.lyubchyk@fct.unl.pt

Authors' contributions

Lyubchyk S.I.: conceptualization, validation, investigation, writing – original draft.
Lyubchyk S.B.: software, validation, formal analysis, investigation, writing – original draft.
Lyubchyk A.: methodology, software, formal analysis, data curation, supervision, writing – review & editing.

Характеризація адсорбційних властивостей діоксиду цирконію при різних положеннях ітрію в ґратці ZrO_2–Y_2O_3

С.І. Любчик, С.Б. Любчик, А.І. Любчик

Анотація. Наведено теоретичні дослідження перерозподілу електричних зарядів у шарі тетрагональної пластини діоксиду цирконію, стабілізованого ітрієм, на основі положення атома ітрію в кристалічній ґратці як для сухої, так і для вологої атмосфери. Для моделювання використовувалася теорія функціоналу щільності з наближенням локальної щільності (DFT-LDA). Проведено розрахунки пошарового розподілу електронної густини по товщині нескінченної пластини 001 тетрагонального діоксиду цирконію, стабілізованого ітрієм, які показали, що зміна положення стабілізуючого атома ітрію та його симетрії в шарі приводить до зміни повної енергії діоксиду цирконію як для сухої поверхні, так і для гідратованої поверхні 001. Установлено, що поверхнева щільність заряду 001-поверхні нескінченної тетрагональної цирконієвої пластини зростає пропорційно ступеню гідратації.

Ключові слова: діоксид цирконію, стабілізований оксидом ітрію; локальний потенціал; повна енергія системи; гідратована поверхня.